EUSIPCO 2013 1569746805

UNMIXING USING A COMBINED MICROSCOPIC AND MACROSCOPIC MIXTURE MODEL WITH DISTINCT ENDMEMBERS

Dmitri Dranishnikov[♯], *Paul Gader*[♯] , *Alina Zare*[*], *Taylor Glenn*[♯]

[♯]Computer and Information Science and Engineering, University of Florida
[*]Electrical and Computer Engineering, University of Missouri

ABSTRACT

Much work in the study of hyperspectral imagery has focused on macroscopic mixtures and unmixing via the linear mixing model. A substantially different approach seeks to model hyperspectral data non-linearly in order to accurately describe intimate or microscopic relationships of materials within the image. In this paper we present and discuss a new model (MacMicDEM) that seeks to unify both approaches by representing a pixel as both linearly and non-linearly mixed, with the condition that the endmembers for both mixture types need not be related. Using this model, we develop a method to accurately and quickly unmix data which is both macroscopically and microscopically mixed. Subsequently, this method is then validated on synthetic and real datasets.

Index Terms— Microscopic, Hyperspectral, Unmixing, BRDF

1. INTRODUCTION

Researchers have focused intensely on the spectral unmixing problem over the past 10-15 years. A majority of this focus has been on unmixing the Linear Mixing Model (LMM) [1]. Consequently, many linear unmixing algorithms achieve very good performance and are well-understood. In spite of receiving less attention, nonlinear unmixing algorithms have been investigated steadily throughout this period. The success in unmixing the LMM and documentation of the non-negligible effects of nonlinearities [2, 3] are sufficient to warrant an increased focus on nonlinear unmixing algorithms.

Recent approaches to non-linear mixing have included kernel-based methods [4, 5], bilinear models, manifold-based methods, and methods based upon physical models [1]. In this paper we focus on a physical-model based approach using the widely known bidirectional reflectance distribution function (BRDF) introduced by Hapke [6]. This function describes the relationship of observed reflectance to the albedo of substances within the scene, based upon the properties of the incident and emergent photons. Several approaches exist that utilize the Hapke BRDF, however only work by Close et al. [7] has come up with a model to take into account simultaneously both linear (Macroscopic) and non-linear (Microscopic) mixing within the same pixel using the BRDF.

In this paper a new non-linear unmixing model MacMicDEM (Macroscopic and Microscopic Difference from linear EndMembers), that expands upon the work in [7], is presented. Following this, estimation techniques for all relevant parameters are derived and experimental results are shown for synthetic and real datasets.

2. MACROSCOPIC AND MICROSCOPIC UNMIXING MODELS

When light is incident on a material, some of the light is scattered and some is absorbed. A commonly used quantity to measure the absorption properties of any such material is known as the single scattering albedo. This can be defined as the ratio of the reduction in radiance due to scattering to the reduction in radiance due to both scattering and absorption. An approximation to Hapke's BRDF model [6] describes the following relationship between albedo and radiance, which we assume has been mapped to reflectance.

$$R_\lambda(w_\lambda) = \frac{w_\lambda}{4(c_i + c_e)}[H(c_i)H(c_e)] \tag{1}$$

Here λ represents wavelength, R represents reflectance as a function of wavelength, c_i, c_e represent the cosines of the angles of incidence and emergence, and H is an approximation of Chandrasekhar's function for isotropic scattering given by

$$H(c) = \frac{1 + 2c}{(1 + 2c(1 - w_\lambda)^{\frac{1}{2}})} \tag{2}$$

where w_λ is the average single scattering albedo (SSA). For a microscopically mixed substance of interest the SSA is defined in terms of constituent material albedos ($w_{m\lambda}$) and corresponding fractional proportions (f_m) as follows [6]:

$$w_\lambda = \sum_{m=1}^{M} f_m w_{m\lambda} \text{ and } \sum_{m=1}^{M} f_m = 1\ ,\ f_m \geq 0 \tag{3}$$

Microscopic mixing can thus be seen to be a linear mixture in the albedo domain (Eqn. 3), which translates to a

nonlinear mixture (via Eqn. 1) in the domain of reflectance. There are many ways to combine Hapke's microscopic mixing model with the linear mixing model to devise nonlinear models for spectral unmixing [7]. We adopt the approach of modeling a pixel in such a way that it can be both partially linearly mixed and partially nonlinearly mixed

$$\mathbf{x}_n = \sum_{m=1}^{M} \alpha_{n,m}\mathbf{e}_m + \alpha_{n,M+1}R(\sum_{m=1}^{M} \mathbf{w}_m f_{n,m}) \quad (4)$$

Which we will also refer to in matrix form as

$$\mathbf{x}_n = \mathbf{E}\boldsymbol{\alpha}_{n,1:M} + \alpha_{n,M+1}R(\mathbf{W}\mathbf{f}_n) \quad (5)$$

Here $\mathbf{x}_n$ is the K-dimensional spectral vector of the $n'th$ pixel ($n \in \{1, ..., N\}$). Similarly, $\mathbf{e}_m$ denotes the spectra of the m-th linear endmember in the reflectance domain and $\mathbf{w}_m$ denotes the spectra of the m-th non-linear endmember in the albedo domain. Corresponding proportions are given by $\alpha_{n,m}, f_{n,m}$ respectively, and are assumed to satisfy positivity and sum to one constraints (Eqns. 7 - 8). Note also that we extend the definition of R_λ in Eqn. 1 to that of a vector function : $R(\mathbf{w}) = [R_\lambda(w_1), ..., R_\lambda(w_K)]$.

The model shown above is similar to the model given by [7]. However, in our method a key assumption made by [7] is not made: The endmembers involved in linear mixing are not assumed to be the related to the endmembers involved in nonlinear mixing. In other words we don't assume

$$R(\mathbf{w}_m) = \mathbf{e}_m. \quad (6)$$

Our observations on real data and the methods used in [7] have indicated that endmembers in hyperspectral data are present as constituents of macroscopic or microscopic mixtures, but often times not both. Indeed, assuming endmembers that are, for example, present in a linear mixture will also be present in a non linear mixture elsewhere in the scene is not a realistic assumption, so we do not enforce this constraint. Subsequently, the complexity of our model is reduced (compared to [7]) : the size of the required endmember set to unmix a given dataset, and thus the number of proportions to estimate, is less. Furthermore, future work into endmember extraction using this model is more feasible as this constraint is mathematically prohibitive.

3. INVERTING THE MACMICDEM MODEL

Now that we have defined our mixing model (Eqn 4), we describe the unmixing process, that is we describe estimation Non-linear proportions ($\mathbf{f}$), and linear proportions $\boldsymbol{\alpha}$. Additionally we perform this estimation under the following constraints, corresponding to physical constraints of linear mixing in the reflectance and albedo domains :

$$\forall i, \sum_{m=1}^{M} f_{i,m} = 1 \text{ and } f_{i,m} \geq 0 \quad (7)$$

$$\forall i, \sum_{m=1}^{M+1} \alpha_{i,m} = 1 \text{ and } \alpha_{i,m} \geq 0 \quad (8)$$

We approach this inversion problem by defining an objective function for purposes of minimization. This objective is based upon the objective introduced by Berman et al. in [8], and consists of a Residual Sum of Squares (RSS) form:

$$RSS := \frac{1}{N}\sum_{n=1}^{N} ||\mathbf{x}_n - \mathbf{E}\boldsymbol{\alpha}_{n,1:M} - \alpha_{n,M+1}R(\mathbf{W}\mathbf{f}_n)||^2 \quad (9)$$

Fixing the non-linear proportions, estimation of $\boldsymbol{\alpha}_n$ is straightforward and can be accomplished by fixing a temporary $M+1$'th endmember : $\mathbf{e}_{M+1} := R(\mathbf{W}\mathbf{f}_n)$. Then we write the RSS as

$$RSS := \frac{1}{N}\sum_{n=1}^{N} ||\mathbf{x}_n - \mathbf{E}'\boldsymbol{\alpha}_n||^2 \quad (10)$$

Where $\mathbf{E}' := [\mathbf{E}, \mathbf{e}_{M+1}]$. The resulting objective is then identical (up to a constant) to that of ICE [8], In other words we have reduced the problem to that of the linear case and unmix accordingly. The standard approach in this case is through quadratic programming (QP), since RSS can be observed to be quadratic in $\boldsymbol{\alpha}$. as in ICE [8].

If, on the other hand, we assume the linear proportions fixed, we can estimate $\mathbf{f}$. However, the function R is nonlinear so the objective is not quadratic in $\mathbf{f}$, so instead we resort to a different objective function by redefining the RSS term as the RSS in the albedo domain :

$$RSS_{alb} := \frac{1}{N}\sum_{n=1}^{N} ||R^{-1}(\frac{\mathbf{x}_n - \sum_{k=1}^{M}\alpha_{nk}\mathbf{e}_k}{\alpha_{n,M+1}}) - \sum_{k=1}^{M} f_{ik}\mathbf{w}_k||^2 \quad (11)$$

Note here that R is monotonic as a function of albedo [6], and thus R^{-1} is well defined. With this objective, the full objective function is quadratic in $\mathbf{f}$, so we again use quadratic programming to estimate the non-linear abundances. It is also worthwhile to know that in the purely non-linear case $\alpha_{n,M+1} = 1$, and thus $\alpha_{n,m} = 0$ for $m \leq M$, so this objective simplifies into

$$RSS_{alb} := \frac{1}{N}\sum_{n=1}^{N} ||R^{-1}(\mathbf{x}_n) - \sum_{k=1}^{M} f_{ik}\mathbf{w}_k||^2 \quad (12)$$

Subsequently, by alternating the two above estimation steps in sequence, we come up with the MacMicDEM unmixing algorithm, shown below.

Algorithm 1 Unmixing MacMicDEM

1. *Initialization*
   - Fix $\alpha_{n,M+1} = 1$ for all n
   - Unmix $\mathbf{f}$ using QP and Eqn. (12)
   - Fix $\mathbf{f}$. Unmix α using QP and Eqn. (10)
2. DO UNTIL Convergence or MAX_ITER
   (a) Solve for α using QP and (10).
   (b) Find a set of pixels $Y := \{\mathbf{x_n}\}$ for which $\alpha_{n+1} > 0.01$
   (c) For each pixel in Y. Solve for $\mathbf{f}$ using QP and (11)
   (d) Check for Convergence of the Global Objective Eqn. (9)
3. END

Where MAX_ITER, is a fixed constant denoting an upper bound for iteration. Experimental results can be found in the following sections.

4. EXPERIMENTAL RESULTS : SYNTHETIC DATA

In this section we describe an experiment on a synthetic dataset generated with endmembers taken from Ground-measured spectra collected over Gulfport, Mississippi in 2010 by Gader et al. of the University of Florida [9].

For the endmembers in our experiment we selected three spectra (Grass, Sidewalk, and a Yellow Curb) for the linear mixture, and three spectra (Sand, Dead Leaves, Dead Weeds) for the non linear mixture. These endmember spectra can be seen in Figure 2.

Concerning construction of the actual dataset, we dimensionally reduced the data to 50 dimensions, and proceeded by taking a dataset of 15000 points consisting of 5000 purely linear, 5000 purely non-linear and 5000 mixed linear and non-linear spectra. For testing purposes we created 1000 such datasets, with varying mixture structure. One such dataset can be seen in Figure 1. Furthermore for all non-linear mixing we set an incidence and emergence angle of 45 degrees, these angles are treated parameters and must be known in advance for the utilization of Hapke's BRDF (Eqn. 1) to be effective.

Proportions for each mixture component were drawn from varied Dirichlet distributions for each of the thousand datasets. Each parameter in the Dirichlet distribution was varied uniformly from 0.1 to 10 over all 1000 generated datasets. This was done with the exception of the mixed portion of each dataset, whose Dirichlet parameter corresponding to α_{M+1}, the non-linear proportion mixture, was fixed to the sum of the Dirichlet parameters for $\alpha_1 ... \alpha_M$ to ensure mixture balance.

Additionally, Gaussian noise with variance 10^{-5} was added to each band of each data point. Table 1 shows the mean result of unmixing MacMicDEM on each portion of

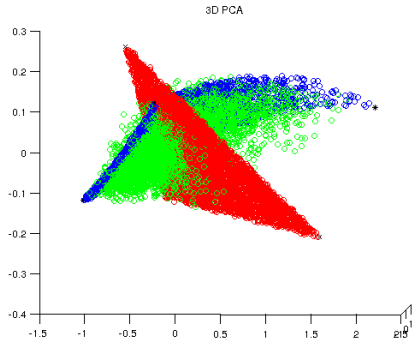

Fig. 1: *This figure is a 3D PCA visualization of a single dataset of 15000 points. Red shows the linear mixture, Blue the non-linear mixture, and Green the combined linear-non-linear mixture.*

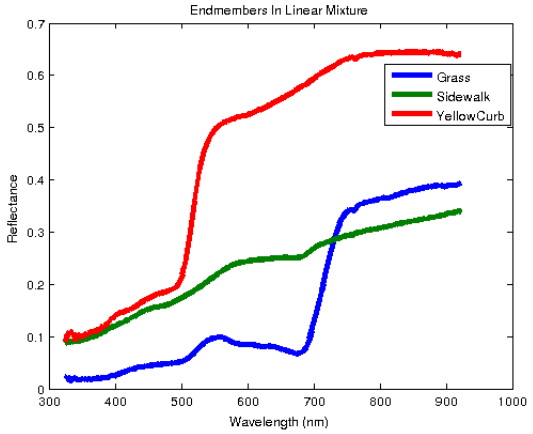

(a)

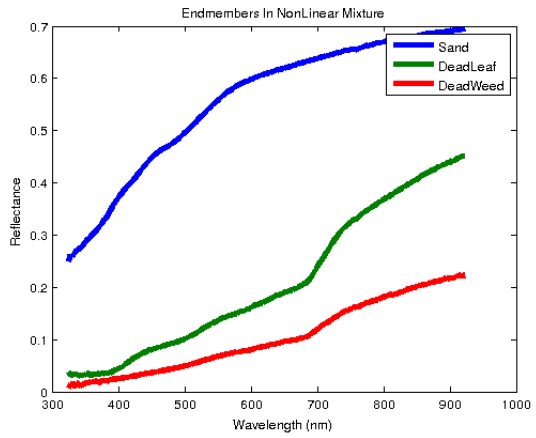

(b)

Fig. 2: *Endmembers for the (a). Linear ($\mathbf{E}$) and (b). Nonlinear ($R(\mathbf{W})$) portions of the model.*

each dataset, and Table 2 shows the corresponding variance of each estimator.

Table 1*: Synthetic Data Results*

Error Measure	Linear	Non-Linear	Mixed
$\mathbf{RSS}/N(10^{-3})$	0.6215	0.5548	0.6132
$\mathbf{RMSE}_F$	-	0.0193	0.1115
$\mathbf{RMSE}_\alpha$	0.0493	0.0206	0.0742
$\mathbf{RMSE}_{\alpha_{M+1}}$	0.0778	0.0321	0.0964

Here the Residual Sum of Squares ($\mathbf{RSS}$) is defined by the quantity that appears in Eqn. (9), and $\mathbf{RMSE_F}, \mathbf{RMSE}_\alpha$ are the root mean squared errors (RMSE) of the linear and non-linear proportions respectively, averaged over each pixel. Furthermore, $\mathbf{RMSE}_{\alpha_{\mathbf{M+1}}}$ is the average RMSE of just the nonlinear proportion $\alpha_{M+1,n}$ over each pixel $\mathbf{x_n}$. Note that value of $\mathbf{f}$ plays no role in the case of a purely linear model (e.g. $\alpha_{M+1,n} < 0.01$) as in the first portion of each dataset, so we omit this result.

Table 2*: Synthetic Variance*

Variance Of	Linear	Non-Linear	Mixed
$\mathbf{RSS}/N(10^{-6})$	0.0195	0.0054	0.0517
$\mathbf{RMSE}_F(10^{-3})$	-	0.0464	2.7248
$\mathbf{RMSE}_\alpha(10^{-3})$	0.0231	0.0504	0.6627
$\mathbf{RMSE}_{\alpha_{M+1}}(10^{-3})$	0.0597	0.1268	1.3120

It can be seen from these results that the model performs best on the purely non-linear portion of the dataset(s), with low $\mathbf{RMSE}$ values for all parameters. Proportion estimates for the mixed and linear portions are higher. Moreover, observe the significantly high variance in the mixed portion of the dataset(s), this variance is several orders of magnitude higher than those of the other portions, even though both the RSS and RSS variance is relatively low. This indicates the possibility that the model contains multiple near-correct solutions, which is a known issue with other models of this type [10]. To confirm this effect we repeated this experiment with a single dataset with no noise. Results can be seen in Table 3.

Table 3*: Synthetic Data : No Noise*

Error Measure	Linear	Non-Linear	Mixed
$\mathbf{RSS}/N(10^{-3})$	0	0	0.1480
$\mathbf{RMSE}_F$	-	0	0.0651
$\mathbf{RMSE}_\alpha$	0	0	0.0708
$\mathbf{RMSE}_{\alpha_{M+1}}$	0	0	0.0826

Where a value of 0 denotes a value that is essentially zero ($< 10^{-13}$). MacMicDEM was able to automatically detect pure linear and pure non-linear mixtures in the case of no noise. This is clear evidence that the model is over-parameterized in the mixed pixel case. Indeed, the high error in the presence of both microscopic and macroscopic mixtures within the same pixel suggests strongly that unmixing via MacMicDEM can be an ill-posed inversion problem with multiple solutions that minimize the objective, although this issue does not appear to affect pixels composed of purely macroscopic or purely microscopic mixtures.

5. EXPERIMENTAL RESULTS : REAL DATA

In this section we describe an experiment on a real-world dataset using data collected over Gulfport, Mississippi in 2010 by Gader et al. of the University of Florida [9]. First, we selected a region of the collection that seemed likely to have intimate mixtures, this region is shown in Figure 3, and comprises a dataset of 3111 pixels with 51 bands each.

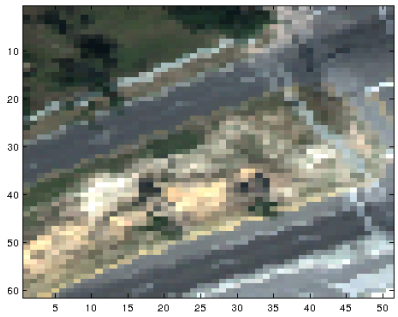

Fig. 3*: This figure shows the region selected for the dataset, this region shows a road, a median, and some sandy and grassy areas.*

For the endmembers in our experiment we selected four Ground-measured spectra (Live Grass, Dead Leaves, Concrete, and Sand), which were scaled appropriately to the dimension of the data. These spectra were selected based upon visual analysis of likely constituents of the scene, and some of them are shown in Figure 2.

When unmixing with MacMicDEM we used Grass, Dead Leaves, Concrete as endmembers for the linear portion of the mixture, and Dead Leaves, Sand, and Grass as endmembers for the non-linear portion. We justify the use of similar endmembers in different parts of the model as a reflection of our understanding of the scene: some endmembers are present in both linear and nonlinear mixtures, but others should not be. We expected to detect a strong non-linear response in the grassy area to the top left (with Grass and Dead Leaves), as well as the median of the road (with Sand, Grass, and Dead Leaves).

For unmixing, we used an angle of incidence of 45, close to the angle of the sun at the time, and an angle of emergence of 10, reflecting the position of this scene to the data collection device. Figure 4 shows the resulting values of $\alpha_{n,M+1}$

for each pixel after unmixing with MacMicDEM.

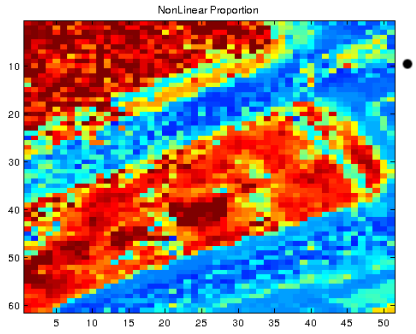

Fig. 4: *This figure shows the strength of the non-linear proportion α_{M+1} over this dataset. Proportion values of 1.0 are shown in red, and 0.0 are shown in blue.*

It can be seen that there is a strong non-linear response in the median, as expected, as well as a response from the grassy area in the top left corner. Figures 5 (a) and (b) show the resulting linear and non-linear proportion maps.

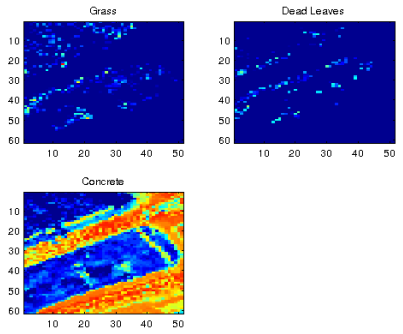

(a)

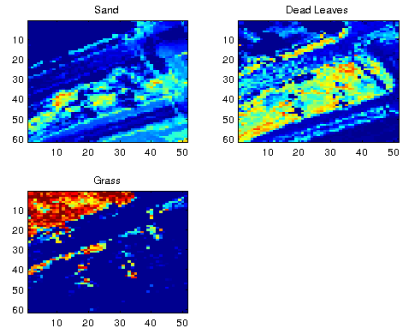

(b)

Fig. 5: *Estimated proportion maps with red denoting a proportion of 1.0 and blue denoting a proportion of 0.0, for (a) the Linear and (b) the Non Linear parts of the model. The non-linear proportion is scaled by the corresponding value of α_{M+1} for each pixel.*

Furthermore, observe that in the non-linear proportion maps there is a non-trivial non-linear response present in the grassy area in the top left from an intimate mixture of both the Dead Leaves and Grass endmember. Likewise, there is a strong non-linear response present in the median between the Sand and Dead Leaves endmembers, indicating the likelihood of intimate mixing between sand and dead vegetation within the median.

6. CONCLUSION AND FUTURE WORK

In conclusion we have presented a novel algorithm, MacMicDEM, for non-linear spectral unmixing of datasets containing both microscopic and macroscopic mixtures and have shown it to be effective at unmixing synthetic data in the case of purely linear and purely non-linear mixtures, but not as effective for data which is both linearly and non-linearly mixed. Moreover, we found this method to be faster than previous approaches of this form such as [7], and it can thus be used on very large datasets. Possibilities for future work in this area could include both linear and non-linear endmember estimation algorithms for this model, as well as the addition of a regularization term for the abundance fractions.

7. REFERENCES

[1] José M. Bioucas-Dias, Antonio Plaza, Nicolas Dobigeon, Mario Parente, Qian Du, Paul Gader, and Jocelyn Chanussot, "Hyperspectral unmixing overview: Geometrical, statistical, and sparse regression-based approaches," *IEEE J. Sel. Topics Appl. Earth Observations Remote Sensing*, 2012, to appear.

[2] T. Han and D.G. Goodenough, "Investigation of nonlinearity in hyperspectral imagery using surrogate data methods," *Geoscience and Remote Sensing, IEEE Transactions on*, vol. 46, no. 10, pp. 2840 –2847, oct. 2008.

[3] N. Keshava and J.F. Mustard, "Spectral unmixing," *Signal Processing Magazine, IEEE*, vol. 19, no. 1, pp. 44 –57, jan 2002.

[4] Jie Chen, Cdric Richard, and Paul Honeine, "Nonlinear unmixing of hyperspectral images with multi-kernel learning," in *Hyperspectral Image and Signal Processing: Evolution in Remote Sensing (WHISPERS), 2012 4rd Workshop on*, 2012.

[5] Jie Chen, Cdric Richard, and Paul Honeine, "Nonlinear unmixing of hyperspectral data based on a linear-mixture/nonlinear-fluctuation model," *Signal Processing, IEEE Transactions on*, vol. 61, no. 2, pp. 480–492, 2013.

[6] Bruce Hapke, *Theory of reflectance and emittance spectroscopy*, Cambridge University Press, 2012.

[7] Ryan Close, Paul Gader, Alina Zare, Joseph Wilson, and Dmitri Dranishnikov, "Endmember extraction using the physics-based multi-mixture pixel model," in *SPIE Optical Engineering+ Applications*. International Society for Optics and Photonics, 2012, pp. 85150L–85150L.

[8] M. Berman, H. Kiiveri, R. Lagerstrom, A. Ernst, R. Dunne, and J.F. Huntington, "Ice: a statistical approach to identifying endmembers in hyperspectral images," *Geoscience and Remote Sensing, IEEE Transactions on*, vol. 42, no. 10, pp. 2085 – 2095, oct. 2004.

[9] P. Gader, R. Close, and A. Zare, "AVIRIS Data Collection over Gulfport, Mississippi," personal communication.

[10] Ryan Close, *Endmember and proportion estimation using physics-based macroscopic and microscopic mixture models*, Ph.D. thesis, UNIVERSITY OF FLORIDA, 2012.